

Magnetic Resonance in  $\text{K}_2\text{CuCl}_4 \cdot 2\text{H}_2\text{O}^\dagger$ 

N. C. FORD, JR.,\* AND C. D. JEFFRIES

Department of Physics, University of California, Berkeley, California

(Received 22 July 1965)

We have observed the microwave electron spin resonance of  $\text{Cu}^{2+}$  and the proton nuclear magnetic resonance in the temperature range  $0.17 \leq T \leq 4.2^\circ\text{K}$  and in fields in the range 3 to 6 kOe for single crystals of  $\text{K}_2\text{CuCl}_4 \cdot 2\text{H}_2\text{O}$ , an ideal Heisenberg insulating ferromagnet with a Curie temperature  $T_c = 1.1^\circ\text{K}$ . The temperature dependence of the magnetization, as measured by the proton-magnetic-resonance field, is in close agreement with the molecular-field model. The dependence of the microwave ferromagnetic resonance on temperature and sample geometry is in agreement with Kittel's equation. Numerous sharp magneto-static modes are observed and compared with the theory of Walker. The ferromagnetic resonance line width has a temperature-independent component of a few Oe, and a temperature-dependent component which narrows from 65 to 1 Oe as the temperature varies from 4.2 to  $0.7^\circ\text{K}$ . From the observed shift in the ferromagnetic resonance below  $0.6^\circ\text{K}$  due to the hyperfine (hfs) field of the copper nuclei, we find that the hfs constant  $A = 1.5 \times 10^{-2} \text{ cm}^{-1}$ . We observe a new type of ferromagnetic resonance induced by a microwave field parallel to the dc field, which we interpret as a "forbidden" hyperfine resonance corresponding to the simultaneous flip of an electron spin and a nuclear spin.

## I. INTRODUCTION

OF the known insulating ferromagnets, only a few, e.g.,  $\text{CrBr}_3$ <sup>1</sup> and  $\text{EuO}$ ,<sup>2</sup> have a readily accessible Curie temperature  $T_c$ ; most often  $T_c$  is below  $1^\circ\text{K}$ , e.g.,  $\text{Dy}(\text{C}_2\text{H}_5\text{SO}_4)_3 \cdot 9\text{H}_2\text{O}$ , with  $T_c = 0.1^\circ\text{K}$ .<sup>3</sup> We have selected  $\text{K}_2\text{CuCl}_4 \cdot 2\text{H}_2\text{O}$ <sup>4-8</sup> for a detailed study by magnetic resonance over a temperature range from well below to well above the Curie temperature. This copper double chloride salt readily grows in single crystals and has a nearly isotropic paramagnetic Curie temperature  $T_c = 1.2 \pm 0.1^\circ\text{K}$  as determined from specific-heat measurements by Miedema *et al.*,<sup>8</sup> who find that the crystal behaves like an ideal Heisenberg ferromagnet with an isotropic exchange of  $J/k = 0.302^\circ\text{K}$ . From low-frequency susceptibility measurements, Van den Broek *et al.*,<sup>7</sup> find that  $T_c = 1.068^\circ\text{K}$ , with the magnetic field along the  $c$  axis and  $T_c = 1.034^\circ\text{K}$  in the  $[010]$  directions.

The crystal structure<sup>9</sup> of  $\text{K}_2\text{CuCl}_4 \cdot 2\text{H}_2\text{O}$  is depicted in Fig. 1. The copper ions form a body-centered cube with a 6% tetragonal distortion along the  $c$  axis. Each copper ion is surrounded by a rhomboid of chlorine ions

in the  $a$ - $b$  plane, and two oxygen atoms along the  $c$  axis. The x-ray data predict that the major axes of all chlorine rhomboids on the cube centers are perpendicular to the major axes of the rhomboids on the cube edges; one expects two magnetic sites. Abe *et al.*<sup>4-6</sup> have observed the microwave paramagnetic resonance of the  $\text{Cu}^{2+}$  ions in this crystal at temperatures above  $1.3^\circ\text{K}$  and find two lines at  $\lambda = 5 \text{ mm}$ ; however at  $\lambda = 3 \text{ cm}$ , they observe only one line with a large anisotropy in linewidth, which is attributed to a pulling together of the two lines by exchange. In our microwave resonance measurements at  $\lambda = 3 \text{ cm}$  and  $T = 4.2^\circ\text{K}$ , obtained by very rapidly cooling the crystals, we see two lines in some crystals (type A), corresponding to two sites with  $g_{11} = 2.06$  and  $g_1 = 2.22$ . However, in other crystals (type B), we find only one resonance line for all orientations, and conclude that all the chlorine rhomboids are parallel; the  $g$  tensor is axially symmetric, the major axis lying along the major axis of the rhomboid, with  $g_{11} = 2.06$  and  $g_1 = 2.22$ , as shown in Fig. 1. The fact that the  $g$  tensor is axial is probably fortuitous, since there is only rhombohedral symmetry about the principal axis. The type A crystals show a peculiar variation of relative intensity of the two lines depending upon the position of the sample in the cavity, suggesting that the two rhomboid orientations are present over macroscopic regions of the crystals rather than alternating between adjacent planes. It is possible that there is a phase transition and that at room temperature there are two inequivalent sites but at low temperature there is only one site.<sup>9a</sup> To summarize, we believe that there is a single magnetic site in a perfect (type B) crystal with  $g_{11} = 2.06$  lying in the  $a$ - $b$  plane; type B crystals were used in our experiments reported in Sec. III.

<sup>†</sup> Supported in part by the U. S. Office of Naval Research and the Atomic Energy Commission.

\* Present address: Physics Department, University of Massachusetts, Amherst, Massachusetts.

<sup>1</sup> J. F. Dillon, Jr., J. Appl. Phys. **33**, 1191S (1962); J. F. Dillon, Jr., and J. P. Remeika, *Magnetic and Electric Relaxation and Resonance*, edited by J. Smidt (North Holland Publishing Company, Amsterdam, 1962), p. 480.

<sup>2</sup> J. F. Dillon, Jr., and C. E. Olsen, Phys. Rev. **135**, A434 (1964).

<sup>3</sup> A. H. Cooke, D. T. Edmonds, C. B. P. Finn, and W. P. Wolf, J. Phys. Soc. Japan **17**, (suppl. B-1) 481 (1962).

<sup>4</sup> H. Abe, K. Ono, I. Hayashi, J. Shimoda, and K. Iwanaga, J. Phys. Soc. Japan **2**, 814 (1954).

<sup>5</sup> K. Ono and M. Ohtsuka, J. Phys. Soc. Japan **13**, 206 (1958).

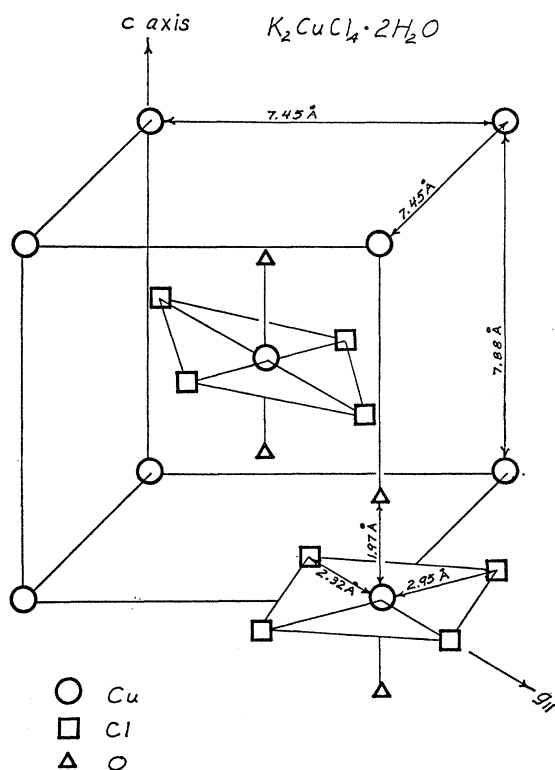
<sup>6</sup> H. Abe, H. Morigaki and K. Koga, Phys. Rev. Letters **9**, 338 (1962); see also W. Low, *Paramagnetic Resonance* (Academic Press Inc., New York, 1963), Vol. II, p. 557.

<sup>7</sup> J. Van den Broek, L. C. Van der Marel, and C. J. Gorter, Physica **27**, 661 (1961).

<sup>8</sup> A. R. Miedema, H. Van Kempen, and W. J. Huiskamp, Physica **29**, 1266 (1963).

<sup>9</sup> S. B. Hendricks and R. G. Dickinson, J. Am. Chem. Soc. **69**, 2149 (1927).

<sup>9a</sup> Note added in proof. Recent measurements by G. Seidel and S. H. Choh (private communication) suggest that the chlorine rhomboid changes into a square as the temperature is slowly varied from 300 to  $77^\circ\text{K}$ , so that the magnetic sites become equivalent at low temperatures. This interpretation is consistent with our observations.

FIG. 1. Crystal structure of  $K_2CuCl_4 \cdot 2H_2O$ .

As discussed more fully in Sec. II, our data are in the usual form of recordings of the microwave power absorbed by the crystal as an external dc field  $H$  is swept through the resonance region. Figures 2, 3, and 4 give a preview of the experimental results and display these general features: Although there is a single magnetic site many lines are observed; e.g., in Fig. 2, line  $a$  is the uniform or Kittel ferromagnetic resonance mode,<sup>10</sup> whereas line  $f$  is a new type of resonance induced by a microwave field parallel to the dc field, thought to be due to a simultaneous electron and nuclear spin flip, nominally forbidden. The resonance lines narrow significantly and shift as the temperature is lowered from  $T=4.2$  to  $T=0.2^\circ K$ . Figure 3 shows the spectra for various values of the angle  $\theta$  between  $H$  and the microwave field  $H_1$ ; for  $\theta=0$ , the  $f$  line is strongest, but for  $\theta \geq 5^\circ$ , it becomes dominated by the  $a$  line plus a number of magnetostatic modes,<sup>11</sup> corresponding to precession of the spins with a macroscopic variation of phase over the sample. These are more clearly shown in Fig. 4. There is no marked change in any of the spectra as the temperature is varied through the Curie temperature. That is, the transition from paramagnetic resonance to ferromagnetic resonance is not well defined because the relatively large field  $H \approx 3$  kOe polarizes the

spins at  $T \sim 1^\circ K$  even in the absence of exchange. Features usually associated with ferromagnetic resonance, e.g., dependence of resonance field on sample geometry, and magnetostatic modes, are also observed in the paramagnetic region above  $T_c$ . Before presenting the detailed results we describe our experimental arrangement.

## II. APPARATUS

The apparatus, shown in Fig. 5, used to observe magnetic resonance between  $0.17$  and  $4.2^\circ K$  is a modified version of that originally described by Ruby *et al.*<sup>12</sup> The crystal sample is attached with silicone vacuum grease to the top of a  $TE_{111}$  mode cylindrical cavity suspended in a vacuum can by a bundle of copper wires, providing a thermal link to a paramagnetic salt pill. This pill,  $150$  g of  $Mn(NH_4)_2(SO_4)_2 \cdot 6H_2O$ , can be put into thermal contact either by a mechanical switch or by helium gas with a reservoir of liquid  $He^4$  at  $1.5^\circ K$ . The cryostat is placed between the poles of a magnet providing a field  $H \leq 10$  kOe. The switch is opened and the entire cryostat raised, thus removing the field from the salt pill, and thereby cooling it and the cavity and sample to  $T=0.17^\circ K$  by adiabatic demagnetization. At this stage the cold cavity is immersed in the field of the magnet, and magnetic

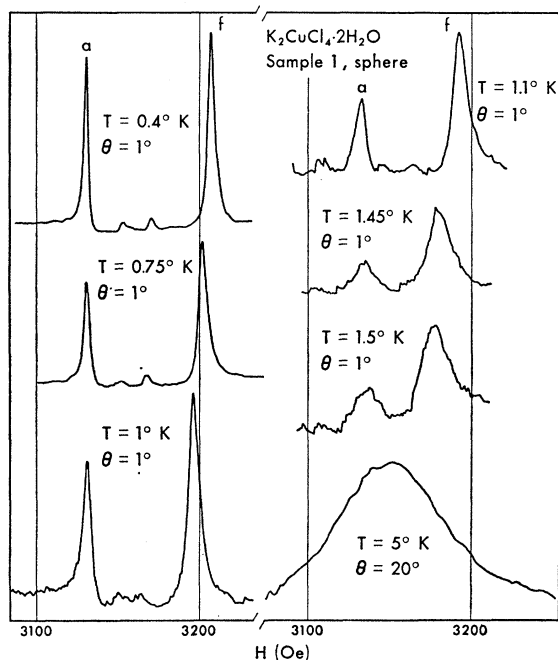


FIG. 2. Magnetic resonance absorption lines observed in a sphere of  $K_2CuCl_4 \cdot 2H_2O$  at  $\nu \approx 9.5$  Gc. Line  $a$  is the uniform precession (Kittel) mode; line  $f$  is a new type of forbidden line thought to correspond to a simultaneous electron and nuclear spin flip; the angle between the dc field and the microwave field is denoted by  $\theta$ .

<sup>10</sup> C. Kittel, Phys. Rev. **73**, 155 (1948).

<sup>11</sup> L. R. Walker, J. Appl. Phys. **29**, 310 (1958).

<sup>12</sup> R. H. Ruby, H. Benoit, and C. D. Jeffries, Phys. Rev. **127**, 51 (1962).

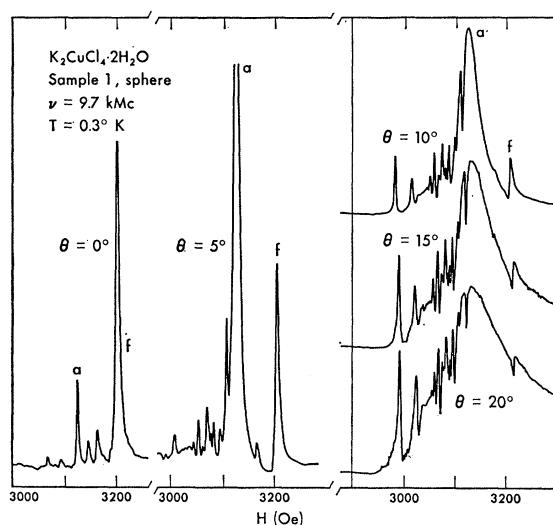


FIG. 3. Magnetic resonance absorption lines, showing dependence on the angle  $\theta$  (see Fig. 2). The numerous sharp lines below line  $a$  are magnetostatic modes.

resonance is observed. The temperature of the cavity is measured by a resistance thermometer, and data are taken over several hours as the cavity warms up to the temperature of the liquid-helium reservoir.

Connected to the cavity are two miniature coaxial cables which are thermally trapped by the salt pill. One cable connects the cavity to the previously described<sup>12</sup> superheterodyne microwave paramagnetic-resonance spectrometer operating at  $\nu \approx 9.5$  Gc. A chart recorder is directly connected to the output of the second detector; this directly records the magnetic-resonance absorption as is shown in Figs. 2, 3, and 4. The other coaxial cable connects a small coil around the sample

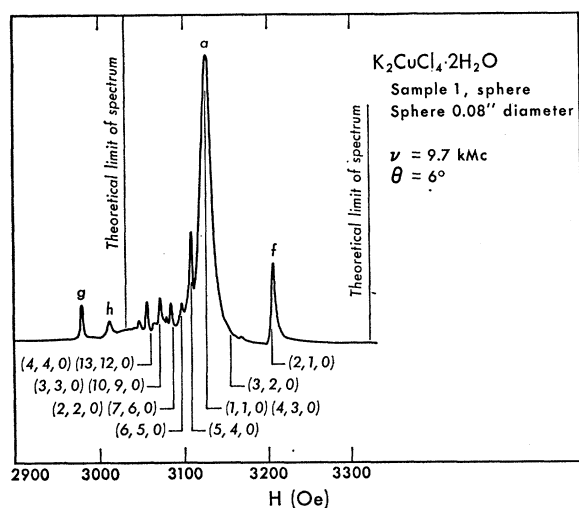


FIG. 4. Magnetic resonance lines observed in a sphere of  $K_2CuCl_4 \cdot 2H_2O$  showing the uniform precession line  $a$ , the forbidden line  $f$ , two lines  $g$  and  $h$  probably due to wall effects, and numerous magnetostatic modes, with the theoretical positions given by Eqs. (14) and (15).

inside the cavity to a nuclear-magnetic-resonance detector of the  $Q$ -meter type, previously described.<sup>13</sup> This was used for observing the proton magnetic resonance in  $K_2CuCl_4 \cdot 2H_2O$ , as will be discussed in Sec. III, in the range  $\nu = 20$  to 42 Mc/sec.

The temperature of the cavity was continuously measured by a Radiation Research Corporation Model CG4A resistance thermometer, consisting of an In- and Sn-doped single crystal of Ge, connected to a sensitive resistance bridge. One of the wire electrodes to the Ge crystal was soldered to the top of the cavity for good thermal contact; the response time of this arrangement is about 3 sec. The calibration of the thermometer was performed as follows. Two small (10 mg) crystals of

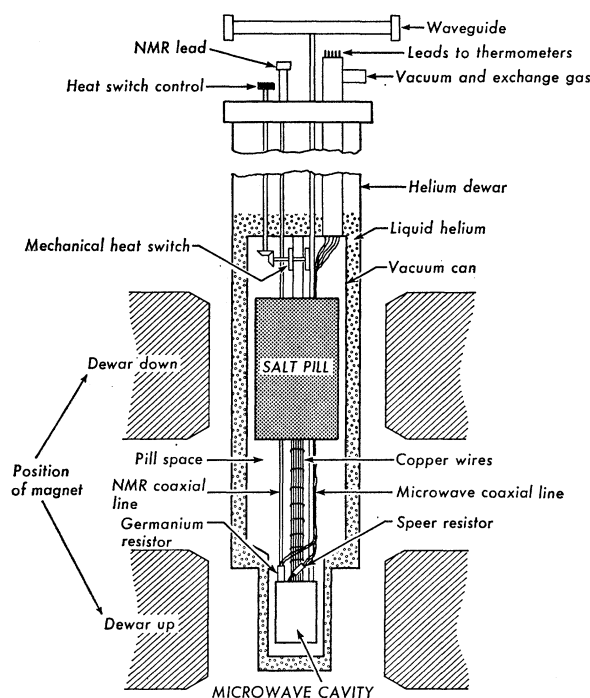


FIG. 5. Microwave magnetic resonance apparatus for use in the range  $1.7 \leq T \leq 4.2^\circ K$ .

1% Nd in  $La_2Mg_3(NO_3)_{12} \cdot 24H_2O$  were mounted in the cavity, one being inside a large single crystal of  $Ce_2Mg_3(NO_3)_{12} \cdot 24H_2O$ . We measured the difference  $\Delta H$  in the microwave paramagnetic-resonance field for the two Nd crystals, which is linearly proportional to the magnetization in the Ce crystal. Since this Ce salt is known to be an ideal paramagnet down to  $0.006^\circ K$ <sup>14</sup> we can write  $\Delta H = D \tanh(g\beta H/2kT)$  from the Langevin-Debye equation for effective spin  $S = \frac{1}{2}$ . The constant  $D$  was determined from measurements in the liquid-helium range, the temperature being taken from the

<sup>13</sup> T. J. Schmugge and C. D. Jeffries, Phys. Rev. **138**, A1785 (1965).

<sup>14</sup> J. M. Daniels and F. N. H. Robinson, Phil. Mag. **44**, 630 (1953).

TABLE I. Characteristics of  $K_2CuCl_4 \cdot 2H_2O$  samples.

Sample No.	Description
1	0.08-in. diam sphere, polished with rouge
2	ellipsoid of revolution, 5/32-in. diam $\times$ 1/32-in. thick, $g_{11}$ in plane
3	ellipsoid, 1/64 in. $\times$ 6/64 in. $\times$ 9/64 in., polished with 7/0-240 sandpaper, $g_{11}$ in plane
4	ellipsoid, 1/64 in. $\times$ 6/64 in. $\times$ 7/64 in., polished with W-509 rouge, $g_{11}$ in plane

vapor pressure. In this way we obtained an empirical expression  $R(T)$  for the Ge resistance over the range  $0.17 < T < 4.2^\circ K$  with an accuracy and reproducibility of better than 1%.

The  $K_2CuCl_4 \cdot 2H_2O$  crystals were grown in an open dish at room temperature from an aqueous solution of KCl and  $CuCl_2$ . The ratio of the two constituents required to grow the mixed crystal is not the stoichiometric ratio; however a growing solution will adjust itself to the proper composition by throwing out  $CuCl_2 \cdot 2H_2O$  crystals, and will then produce good crystals of  $K_2CuCl_4 \cdot 2H_2O$  which are usually polyhedral with all axes of approximately equal length. Altogether, four samples were used and are listed in Table I; discs had rounded edges to approximate an ellipsoid. Professor M. Date of Osaka University kindly supplied us with a large single crystal from which samples No. 1 and 4 were cut.

### III. EXPERIMENTAL RESULTS AND INTERPRETATION

#### A. Measurement of the Magnetization

Perhaps the most fundamental of all magnetic measurements is that of the magnetization  $M(T)$ . Heller and Benedek,<sup>15</sup> for example, have shown that nuclear magnetic resonance can provide very accurate values of the zero-field magnetization near the Curie point. Their findings both for ferro- and antiferromagnets show that the molecular-field model does not yield very accurate predictions for the magnetization. However, in our case the presence of the relatively large field  $H$  should enhance the validity of this model considerably. We have measured  $M(T)/M_0$ , the ratio of the magnetization to its saturation value, for  $K_2CuCl_4 \cdot 2H_2O$  by observing the temperature dependence of the proton-nuclear-magnetic-resonance field  $H_{res}$  in sample No. 1, a sphere. Since the demagnetizing field is cancelled by the Lorentz field the net local field  $H_{loc}$  at a proton site is the sum of the applied field and the dipolar fields of the  $Cu^{2+}$  ions within the Lorentz sphere. Since the copper ions have a large exchange, their spins flip at a rapid rate and their dipolar field at the proton site is proportional to the time average of the electron

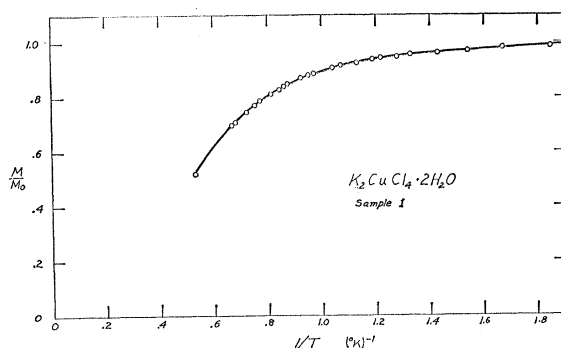


FIG. 6. The magnetization in a sphere of  $K_2CuCl_4 \cdot 2H_2O$  obtained from Eq. (2), using the observed proton resonance field  $H_{res}(T)$  at  $\nu = 33.7$  Mc/sec.

spin  $\langle S_z \rangle$ , which is just proportional to the magnetization  $M$ ; thus

$$H_{loc} = H_{res} + H_d(M/M_0) = 2\pi\nu/\gamma, \quad (1)$$

where  $\nu$  is the proton-magnetic-resonance frequency and  $\gamma = 2\pi \times 42.5$  Mc/sec is the proton gyromagnetic ratio. In an experiment at  $\nu = 33.73$  Mc/sec and  $T = 0.33^\circ K$ , where  $M/M_0 \approx 1$ , we observed  $H_{res} = 6515$  Oe, yielding  $H_d = 1407$  Oe from Eq. (1). The magnetization was then found from

$$M(T)/M_0 = [2\pi\nu/\gamma - H_{res}(T)]/1407, \quad (2)$$

by observing the resonance field  $H_{res}(T)$  over the range  $0.28 \leq T \leq 1.9^\circ K$ . The results are shown in Fig. 6. In the following sections we sometimes use these data to convert measured temperatures to  $M(T)/M_0$ , and then use the latter as an independent variable.

We compare Fig. 6 with that expected from the molecular-field model. For a spin  $S = \frac{1}{2}$  the Langevin-Debye expression for the magnetization including the Weiss field  $\lambda M$  is

$$M/M_0 = \tanh[g\beta(H + \lambda M)/2kT]. \quad (3)$$

By introducing  $\lambda = 2kT_c/g\beta M_0$ , the relation between the Weiss constant and the Curie temperature required to yield the Curie-Weiss law,<sup>16</sup> we can rewrite Eq. (3) as

$$\frac{1}{T} = \frac{1}{T_c} \frac{\tanh^{-1}(M/M_0)}{g\beta H/2kT_c + M/M_0}, \quad (4)$$

from which  $T^{-1}$  may be calculated and plotted as a function of  $M/M_0$ . The saturation magnetization  $M_0 = \frac{1}{2}N g\beta$  has the values 43.2 and 46.5 Oe in the  $g_{11}$  and  $g_4$  directions, respectively, for  $K_2CuCl_4 \cdot 2H_2O$ . In Fig. 7 we compare  $M/M_0$  calculated in this fashion (assuming  $T_c = 1.10^\circ K$  and  $H_{res} = 6800$  Oe) with the data of Fig. 6. Although there is an error of about 3% introduced by assuming  $H_{res}$  to be constant, the agreement is surprisingly good. More exact comparison is made by using

<sup>15</sup> P. Heller and G. B. Benedek, Phys. Rev. Letters 14, 71 (1965).

<sup>16</sup> C. Kittel, Introduction to Solid State Physics (John Wiley & Sons, Inc., New York, 1956), 2nd ed., p. 403.

TABLE II. Values of  $T_c$  calculated from Eq. (4) using measured values of  $H$ ,  $T$ , and  $M/M_0$  from Fig. 6.

$H_{res}$ Oe	$1/T$ (°K) <sup>-1</sup>	$M/M_0$	$T_c$ °K
6518	2.63	0.997	0.793
6600	1.22	0.939	1.015
6704	0.92	0.865	1.10
6818	0.77	0.784	1.145
6928	0.68	0.706	1.140
7196	0.53	0.516	1.095

the measured values of  $T$ ,  $H = H_{res}$ , and  $M/M_0$  in Eq. (4) to calculate an effective Curie temperature. These values, given in Table II, are in good agreement with the specific-heat<sup>8</sup> and susceptibility<sup>7</sup> measurements.

### B. Uniform Precession Mode

In this section we present and interpret data on the dependence of the microwave resonance field on temperature and sample geometry. Kittel<sup>10</sup> first derived the now familiar expression for the uniform precession mode of magnetic resonance in an ellipsoidal body,

$$\omega/\gamma = \{[H + 4\pi M(N_x - N_y)][H + 4\pi M(N_y - N_z)]\}^{1/2}, \quad (5)$$

where  $N_i$  are the demagnetizing factors,  $\gamma = g\beta/\hbar$ ,  $H$  is

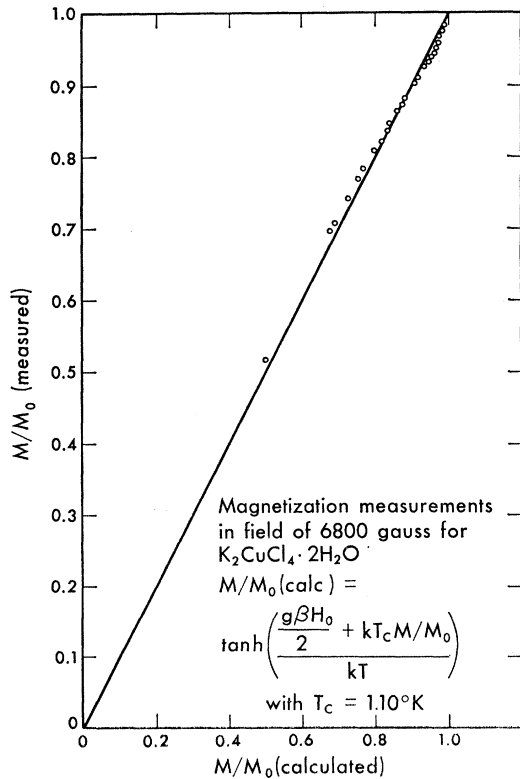


FIG. 7. Comparison of  $M/M_0$  from Fig. 6 to the value calculated from Eq. (4), showing good agreement with the molecular-field model.

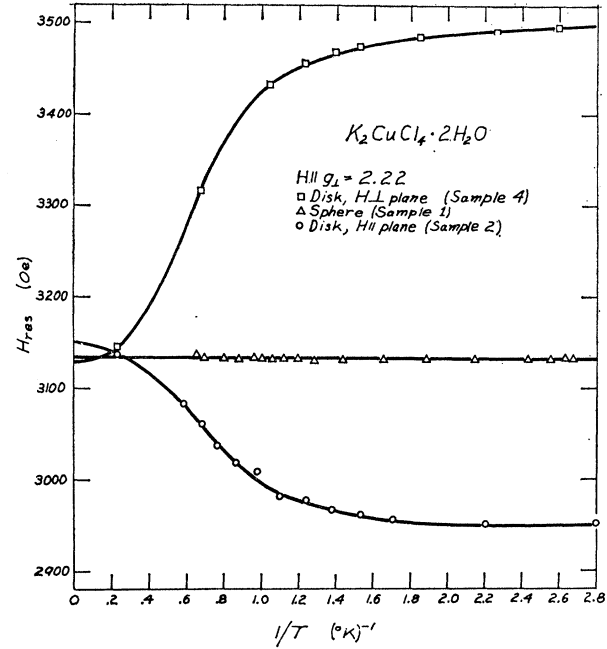


FIG. 8. Microwave-magnetic-resonance field at  $\nu \approx 9.5$  Gc for various sample geometries of  $K_2CuCl_4 \cdot 2H_2O$ , showing the shift with temperature.

the dc resonance field applied in the  $z$  direction, and  $\omega$  is frequency of the driving oscillator. Kittel also showed that the effect of magnetic anisotropy energy can be included in Eq. (5) by a suitable modification of  $N_i$ . For a sample with uniaxial or cubic anisotropy magnetized along the easy axis, the quantity  $2K_1/4\pi M^2$  is added to both  $N_x$  and  $N_y$ . The effective anisotropy field  $H_a = 2K_1/M$  can be readily measured in a spherical sample since  $N_x = N_y = N_z = \frac{1}{3}$  and Eq. (5) becomes

$$\omega/\gamma = H + H_a. \quad (6)$$

For anisotropy due to either anisotropic exchange or dipolar interaction, which are the only types expected in  $K_2CuCl_4 \cdot 2H_2O$ , in the molecular-field approximation we can write  $H_a = 2K_0 M/M_0^2$ , where  $K_0$  is the anisotropy energy at  $T=0$ ; it may be determined by measuring the shift in the resonance line between  $T=0$  and  $T=\infty$ . A resonance experiment was performed on the spherical sample No. 1 over the temperature range  $0.3 \leq T \leq 4.2^\circ\text{K}$  at  $\nu = 9.5$  Gc, and  $H \parallel g_1$ , with the result (see Fig. 8) that a small shift of 7 Oe is observed. Unfortunately, a shift of approximately this size is also expected because of the small deviation from sphericity of the sample. Thus we are only able to say that the anisotropy field  $H_a$  is small, less than  $\sim 10$  Oe.

We found that at temperatures below  $0.6^\circ\text{K}$ , where the magnetization becomes essentially saturated, the resonance field for the uniform mode continued to shift according to the empirical relation

$$\Delta H = H(T = \infty) - H(T) = 2/T \text{ Oe}, \quad (7)$$

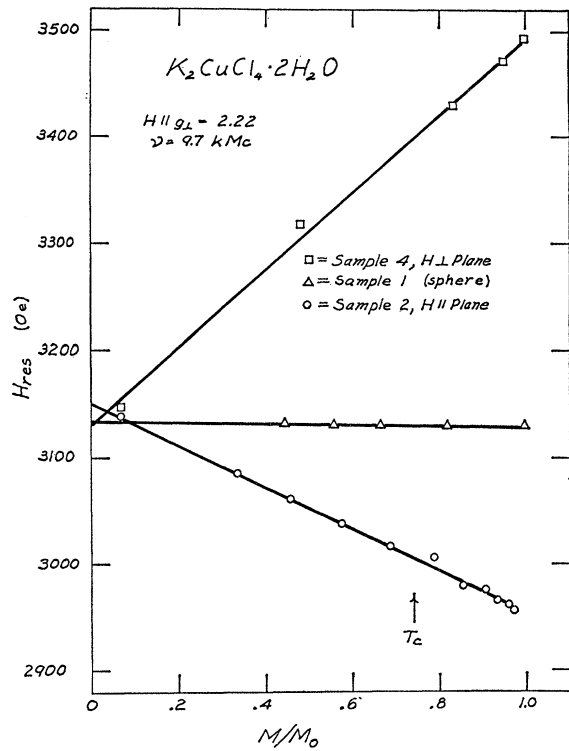


FIG. 9. A replot of the data of Fig. 8 using Fig. 6 to convert  $T$  to  $M/M_0$ . The straight lines are expected from Kittel's equation [Eqs. (6), (12), and (13)].

with  $H$  in the  $g_1$  direction. This shift was found to be independent of sample geometry. We interpret it as arising from the effective field on the electron spins due to the polarization of the copper nuclei by the hyperfine (hfs) interaction  $A\mathbf{I}\cdot\mathbf{S}$ . It is similar to the Overhauser<sup>17</sup> shift in alkali metals observed by Gueron and Rytter,<sup>18</sup> except that here the nuclear polarization is due to a low lattice thermodynamic temperature rather than to dynamic polarization. The shift will be given approximately by

$$\Delta H = A \langle I_z \rangle / g\beta, \quad (8)$$

where the expectation value of the  $z$  component of the nuclear spin is given by

$$\langle I_z \rangle = I(I+1)g_n\beta H_{\text{eff}}/3kT. \quad (9)$$

Here  $H_{\text{eff}}$  is the effective field on the copper nuclei, given to a good approximation by  $H_{\text{eff}} = A \langle S_z \rangle / g_n\beta \cong AS/g_n\beta$  at low temperatures where the electrons are well polarized. Thus

$$\Delta H = I(I+1)SA^2/3kTg\beta, \quad (10)$$

which yields, from Eq. (7) and the appropriate values  $S = \frac{1}{2}$ ,  $g = g_1 = 2.2$ , and  $I = \frac{3}{2}$  for  $\text{Cu}^{63}$  and  $\text{Cu}^{65}$ , the value

$$A = 1.5 \times 10^{-2} \text{ cm}^{-1}. \quad (11)$$

TABLE III. Comparison between the measured field shift (Fig. 5) and calculated shift [Eqs. (12) and (13)] of the uniform precession mode between  $T = 0.5^\circ\text{K}$  and  $T = 4.2^\circ\text{K}$ .

Sample No.	Orientation	Measured shift Oe	Calculated shift Oe
1	$H \parallel g_1$	12	0
2	$H \parallel g_{11} \parallel \text{plane}$	175	169
2	$H \parallel g_1$	195	183
4	$H \parallel g_1 \parallel \text{plane}$	364	380

Actually the hfs is slightly anisotropic, as will be discussed in Sec. III.E, and Eq. (11) is the value in the  $g_1$  direction.

In contrast to the spherical sample, the resonance fields observed for the disc samples vary markedly with temperature, as shown in Fig. 8. For an ellipsoid of revolution with  $H$  along the axis, Eq. (5) becomes

$$H = \omega/\gamma - 4\pi M(N_x - N_y), \quad (12)$$

whereas with  $H$  perpendicular to the axis and  $H \gg 4\pi M$ , we obtain

$$H \cong \omega/\gamma - 2\pi M(N_y - N_z). \quad (13)$$

Using the measured values of  $M(T)/M_0$  from Fig. 6 we have replotted the data of Fig. 8 in Fig. 9, using  $M/M_0$  as the independent variable. This figure shows that the resonance shifts depend linearly on  $M$  as predicted by Eqs. (12) and (13). In fact, a comparison, Table III, between the measured slopes of Fig. 9 and those calculated from Eqs. (12) and (13) using known sample shapes and demagnetizing factors,<sup>19</sup> does show acceptable agreement; the discrepancies are most likely due to uncertainty in demagnetization factors, since the samples are only approximately ellipsoidal.

### C. Magnetostatic Modes

Walker<sup>11</sup> has calculated the resonance fields for higher modes of oscillation of the magnetization in a sphere, in which the phase of  $M(t)$  varies in a definite configuration over the sample. In his notation the resonance fields for two series of these magnetostatic modes are given by

$$H = \omega/\gamma + 4\pi M[N_z - m/(2m+1)] \quad \text{for } (m, m, 0) \text{ modes}, \quad (14)$$

$$H = \omega/\gamma + 4\pi M[N_z - m/(2m+3)] \quad \text{for } (m+1, m, 0) \text{ modes}. \quad (15)$$

The (1,1,0) mode is the Kittel uniform precession, Eq. (5). It can be shown that the entire magnetostatic mode spectrum, including both surface and volume modes, is contained in the interval

$$\omega/\gamma + 4\pi M(N_z - \frac{1}{2}) \leq H \leq \omega/\gamma + 4\pi MN_z. \quad (16)$$

<sup>17</sup> A. W. Overhauser, Phys. Rev. **92**, 411 (1953).

<sup>18</sup> M. Gueron and Ch. Rytter, Phys. Rev. Letters **3**, 338 (1959).

<sup>19</sup> B. Lax and K. J. Button, *Microwave Ferrites and Ferromagnetics* (McGraw-Hill Book Company, Inc., New York, 1962).

For our sample with  $M \rightarrow M_0$ , we thus expect the entire spectrum to be 290 Oe wide.

Magnetostatic modes have been observed in  $K_2CuCl_4 \cdot 2H_2O$  by Abe *et al.*<sup>6</sup> in the paramagnetic region. We have made measurements on our spherical sample No. 1 down to 0.2°K where we find numerous sharp magnetostatic modes as shown in Fig. 3, and in more detail in Fig. 4. The theoretical resonance fields computed from Eqs. (14) and (15) are shown, and compare favorably with the observed resonances. There are, however, three lines *g*, *h*, and *f* in Fig. 4 that cannot be understood on the basis of magnetostatic mode theory, the two most obvious being *g* and *h* lying well below the theoretical limit. These two lines are similar in both amplitude and position to lines observed by Chiba<sup>20</sup> in a sphere of yttrium iron garnet. He attributes them to a magnetic image in the cavity wall and shows that they are dependent on the distance between sample and wall; we suggest that *g* and *h* have a similar origin.

Although line *f* is near the (2,1,0) mode, it is found to be distinct from it and to behave differently from all the other lines: line *f* has a maximum amplitude for  $H \parallel H_1$ , whereas all the other lines have essentially zero intensity for this orientation. In Sec. III.E we suggest that *f* is a forbidden hfs line.

#### D. Line-Width Measurements

We have measured the full linewidth  $\Delta H$  at half-maximum for the uniform precession line *a* and the line *f* for the spherical sample No. 1 over the temperature range  $0.2T \leq 4.2^\circ K$ . The data were taken with  $\theta = \angle H, H_1 \approx 1^\circ$ ; at this orientation the lines *a* and *f* are approximately equal in amplitude (see Fig. 2) and there are relatively few magnetostatic modes. The experimental results are given in Fig. 10 and show a remarkable narrowing at the low temperatures. In the temperature range  $0.2T \leq 0.5^\circ K$  we found a residual temperature-independent linewidth:  $\Delta H_0 = 2.8$  Oe for line *a*;  $\Delta H_0 = 4.5$  Oe for line *f*. This residual width is probably due to magnon interactions at surface imperfections such as have been observed in yttrium iron garnet.<sup>21</sup> This is further supported by the fact that we do observe the residual width to depend on surface polishing; sample No. 3 polished with fine sandpaper showed  $\Delta H_0 = 11$  Oe, whereas sample No. 4 polished with W509 rouge showed  $\Delta H_0 = 1.5$  Oe.

In order to consider separately the temperature-dependent part  $\Delta H(T)$  of the linewidth we have assumed a Lorentzian line shape, as is usual for ferromagnets, and have simply subtracted  $\Delta H_0$  from the measured linewidth, since the convolution of two Lorentzian lines is a Lorentzian line with a width equal to the sum of the two component widths. The result is shown in Fig. 11; the data for both line *a* and line *f* are

<sup>20</sup> Shu Chiba, Appl. Phys. Letters 5, 176 (1964).

<sup>21</sup> R. C. Le Craw, E. G. Spencer, and C. S. Porter, Phys. Rev. 110, 1311 (1958).

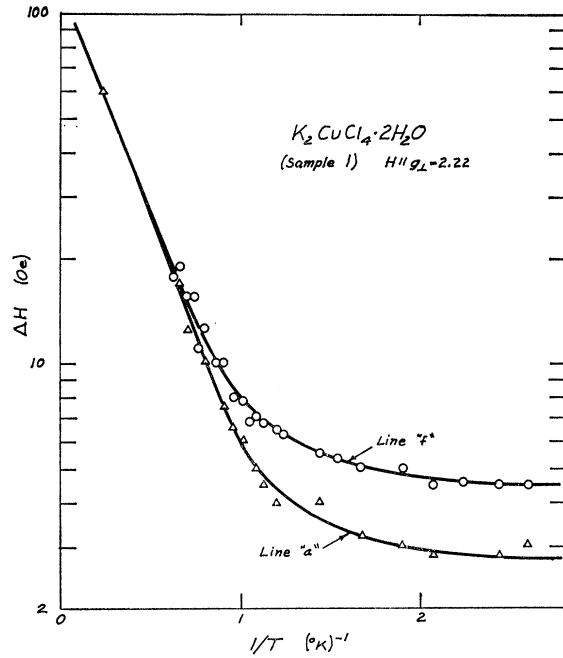


FIG. 10. Linewidth at half-maximum observed in a sphere of  $K_2CuCl_4 \cdot 2H_2O$  versus  $1/T$ .

fit by the empirical expression

$$\Delta H(T) = \Delta H_{\text{meas}} - \Delta H_0 = 145 \exp(-3.7/T) \text{ Oe}, \quad (17)$$

in the region  $0.2T_c \leq T \leq 4T_c$ . There is little experimental or theoretical work to which we might compare this result if we consider only insulating ferromagnets. Dillon and Remeika<sup>1</sup> have published data on the ferromagnetic resonance linewidth in  $CrBr_3$ , for which  $T_c = 32.5^\circ K$ . We compare their data to ours by assuming that  $\Delta H \propto g^2/r_{nn}^3$ , where *g* is the electronic *g* factor and  $r_{nn}$  is the distance between nearest magnetic ions. A plot of  $\Delta H_{\text{meas}}(r_{nn}^3/g^2)$  versus  $T/T_c$  for  $CrBr_3$  is in fair agreement with a similar plot for  $K_2CuCl_4 \cdot 2H_2O$ . This agreement is rather surprising since the difference in exchange constants by a factor of more than 30 would lead us to expect that the  $CrBr_3$  line would be "exchanged narrowed" to a greater extent than our line. However, no general line-width theory applicable to the present case appears to have been published as yet.

#### E. Ferromagnetic-Resonance Hyperfine Line

We review the experimental features of line *f* (see Figs. 2 and 3): The intensity is proportional to  $\cos^2\theta$ , where  $\theta$  is the angle between *H* and the microwave field, in contrast to the uniform precession line *a* and the magnetostatic modes, which follow the usual  $\sin^2\theta$  dependence for magnetic dipole transitions. The spacing  $H_f - H_a$  between *f* and *a* is found to increase as the temperature decreases, and is given by the empirical relation

$$H_f - H_a = 12 + 68M(T)/M_0 \text{ Oe}. \quad (18)$$

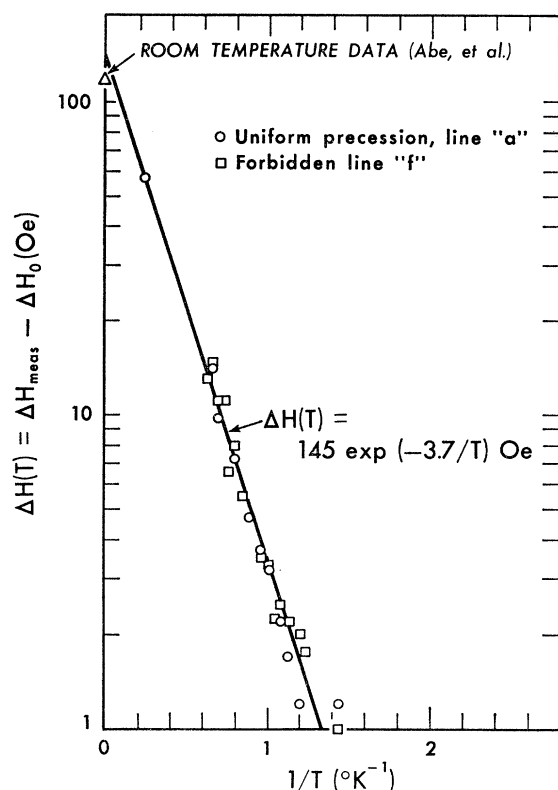


FIG. 11. The temperature-dependent part of the linewidth  $\Delta H(T)$ , obtained by subtracting from the data of Fig. 10 the residual temperature-independent part  $\Delta H_0 = 2.80$  Oe for line  $a$  and  $\Delta H_0 = 4.50$  Oe for line  $f$ .

This relation was verified at frequencies  $\nu = 8.9, 11.7$ , and  $17.3$  Gc with  $H \parallel g_1$  and  $T = 1.5^\circ\text{K}$ ; this experiment excludes the possibility that  $a$  and  $f$  are due to two slightly different ionic  $g$  factors, since the separation is proportional to the magnetization rather than the field. The actual temperature dependence of the resonance fields is given in Fig. 12, where the temperature has been converted to  $M(T)$  by use of Fig. 6. It is clear that the 12-Oe separation in Eq. (18) at  $M/M_0 = 0$  is a gross extrapolation and we do not put much credence in this value. In a sphere line  $f$  lies close to the theoretical position of the  $(2,1,0)$  magnetostatic mode. To eliminate the possibility that  $f$  is a magnetostatic mode, resonance was also observed in a disc, sample No. 4; the uniform precession mode was observed at  $(\omega/\gamma) + 380$  Oe and line  $f$  at  $(\omega/\gamma) + 453$  Oe, whereas the theoretical magnetostatic mode limit occurs at  $(\omega/\gamma) + 446$  Oe. The separation between lines  $a$  and  $f$  was always found to be independent of sample geometry. However, the  $f$  line was found to be observable only when the applied field was almost parallel to the axis of the disc. As the angle  $\varphi$  between the field and the axis was increased, the line broadened, being about 2 Oe at  $\varphi = 0$  and 20 Oe for  $\varphi = 5^\circ$ . The width of the  $a$  line increased by less than a factor of 2 in the same experiment. Finally an attempt

was made to measure the relative intensity of lines  $a$  and  $f$  at several frequencies in the range  $8 \leq \nu \leq 18$  Gc at  $T = 1.4^\circ\text{K}$  for sample No. 1. If we define  $I_f = I_{f0} \cos^2\theta$  and  $I_a \sin^2\theta$ , the measured intensity ratio can be expressed approximately as

$$I_{f0}/I_{a0} \sim 10^{-7} \nu^{4 \pm 1}, \quad (19)$$

where  $\nu$  is in Gc. However, this experiment was not repeated, and Eq. (19) cannot be claimed to be a completely reliable experimental result.

Except for the data on frequency dependence, Eq. (19), all the foregoing features of line  $f$  are explicable by a simple phenomenological model of hfs coupling between the copper ions and the copper nuclei, as indicated schematically in Fig. 13. We first review the "paramagnetic" case of an isolated, magnetically dilute  $\text{Cu}^{2+}$  ion of spin  $S = \frac{1}{2}$  in hfs coupling  $A\mathbf{I} \cdot \mathbf{S}$  with its nucleus of spin  $I = \frac{3}{2}$ ;  $\text{Cu}^{63}$  and  $\text{Cu}^{65}$  will be assumed to be identical, since their magnetic moments differ by only 6%. The energy levels in a large magnetic field are shown in Fig. 13(a), along with the usual paramagnetic resonance hfs lines  $H_1, H_2, H_3$ , and  $H_4$  induced by a microwave field perpendicular to the dc field, and obeying the selection rule  $\Delta m_S = 1, \Delta m_I = 0$ . However, the hfs term  $A\mathbf{I}_+ \mathbf{S}_-$  admixes the zero-order states slightly so that the "forbidden" transitions  $H_{12}, H_{23}$ , and  $H_{34}$  can be induced by a microwave field parallel to

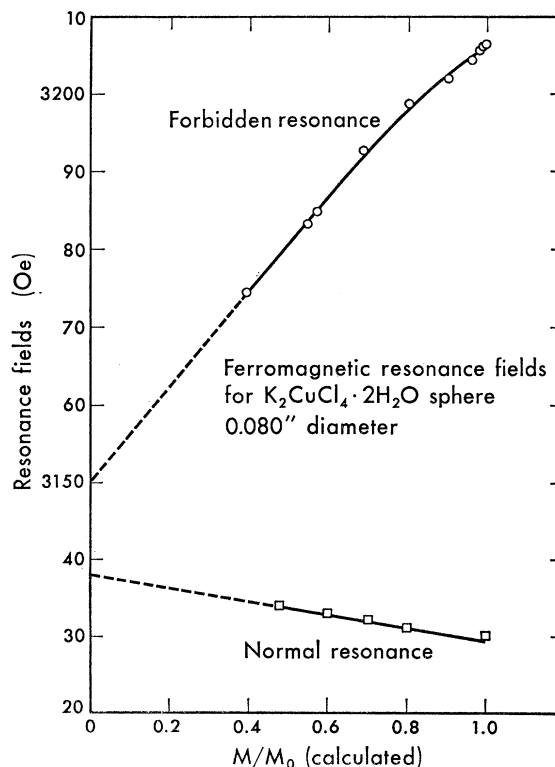


FIG. 12. The observed resonance fields of the normal uniform-mode line  $a$  and the forbidden line  $f$  as a function of  $M/M_0$ , obtained from Fig. 6 and the measured temperature.



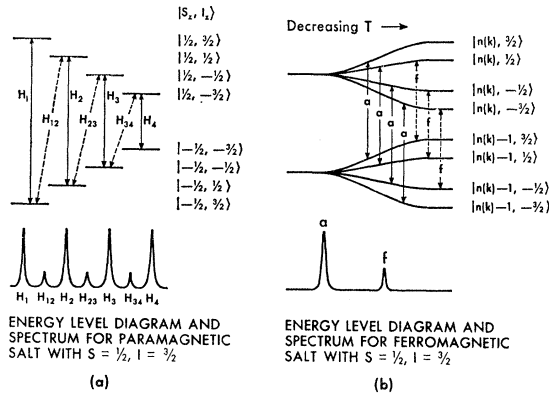


FIG. 13. Schematic energy-level diagram and hfs transitions for (a) a dilute paramagnetic salt, (b) a ferromagnetic salt.

the dc field, weaker than the main line by the factor  $(A/g\beta H)^2 \propto \nu^{-2}$ ; these transitions obey the selection rule  $\Delta m_S = 1$ ,  $\Delta m_I = -1$ .

A somewhat analogous situation can be imagined in a ferromagnet, or in any periodic, magnetically concentrated, well polarized system. There are however striking differences. In the first place, we can no longer think of the electron spin as being localized on a  $Cu^{2+}$  ion, but instead must consider the resonance as the excitation of spin waves of momentum  $k=0$ , distributed throughout the crystal. Thus, if we consider an electron spin state as the set of magnon occupation numbers  $n(k)$ , the ordinary uniform mode of ferromagnetic resonance is a transition between the states  $|n(0), \sum n(k)\rangle$  and  $|n(0)+1, \sum n(k)\rangle$ . Now if we further consider the hfs coupling, we see that on the average the nuclei are all coupled in the same way to the various electron spin states, so that the effect is to split each level into  $2I+1$  levels characterized by  $m_I = \frac{3}{2}, \dots, -\frac{3}{2}$ , as shown in Fig. 13(b). Again there are four allowed transitions  $a$  of the type  $\Delta n(0)=1$ ,  $\Delta m_I=0$  corresponding to the uniform mode; and three transitions  $f$  of the type  $\Delta n(0)=1$ ,  $\Delta m_I=1$ . However, all  $a$  transitions have the same frequency, as do all  $f$  transitions, so that there are only two different resonance lines. If we consider the hfs interaction as a perturbation on the spin-wave functions, and expand in spin-wave operators, we have

$$AI \cdot S = AI_z \langle S_z \rangle + \sum_k (S/2N)^{1/2} (e^{ik \cdot R} a_k I_- + \text{c.c.}), \quad (20)$$

from which we see that the first-order correction to the energy levels is given by  $AI_z \langle S_z \rangle = AI_z SM/M_0$ , which depends on the temperature in the same way as the magnetization. Thus for a spherical sample with no anisotropy field, we might expect two lines: the usual uniform mode line  $a$  at a resonance field independent of temperature, and the line  $f$  at a resonance field higher by  $ASM(T)/g\beta M_0$ , which just becomes  $A/2g\beta$  for  $T \leq 0.5^\circ K$ . This is essentially what we observe. We actually find that the separation between the lines is slightly anisotropic and can be fitted to the axially symmetric hfs interaction  $AI_x S_x + B(I_x S_x + I_y S_y)$ , with

$$\begin{aligned} A &= 0.019 \pm 0.002 \text{ cm}^{-1}, \\ B &= 0.0155 \pm 0.0004 \text{ cm}^{-1}. \end{aligned} \quad (21)$$

The  $z$  axis of the hfs interaction is parallel to the  $z$  axis of the  $g$  tensor. We note that this value of  $B$  is in excellent agreement with Eq. (11).

To summarize, we feel that the experimental evidence on the line  $f$  leads to its interpretation as a "forbidden" hfs ferromagnetic resonance corresponding to a simultaneous electron and nuclear spin flip, in agreement with our tentative earlier report.<sup>22</sup> However, the intensity ratio  $\propto \nu^4$  of Eq. (19) is in marked contrast to the  $\nu^{-2}$  dependence in the paramagnetic case and suggests that the forbidden line is allowed in second-order perturbation theory in an expansion in which the Zeeman energy appears in the numerator rather than in the denominator. However, we have been unable to construct a formal theory that will predict a  $\nu^4$  frequency dependence.

It is worth noting that microwave saturation of the forbidden  $f$  line should lead to a dynamic polarization of the copper nuclei, in analogy to the paramagnetic case<sup>23</sup> and to the Overhauser effect in ferromagnets.<sup>24</sup> This would be particularly applicable to ferromagnets and to magnetically concentrated paramagnets. We have attempted such an experiment with  $K_2CuCl_4 \cdot 2H_2O$ , but were not successful because we were unable to see the copper nuclear resonance.

<sup>22</sup> N. C. Ford, Jr., and C. D. Jeffries, Bull. Am. Phys. Soc. **9**, 739 (1964).

<sup>23</sup> C. D. Jeffries, Phys. Rev. **117**, 1056 (1960).

<sup>24</sup> T. Oguchi and F. Keffer (private communication).